

文章编号:1009-9603(2020)01-0113-07

DOI:10.13673/j.cnki.cn37-1359/te.2020.01.017

# 低渗透油藏CO<sub>2</sub>驱试井解释方法

苏玉亮<sup>1</sup>,蔡明玉<sup>1</sup>,孟凡坤<sup>2</sup>,范理尧<sup>1</sup>,李蕾<sup>1</sup>

(1. 中国石油大学(华东)石油工程学院, 山东 青岛 266580; 2. 中国石油大学胜利学院, 山东 东营 257061)

**摘要:**针对低渗透油藏CO<sub>2</sub>驱试井解释方法不清晰的问题,基于多区复合模型渗流理论,考虑低渗透油藏存在启动压力梯度与压力敏感以及CO<sub>2</sub>驱替过程中流体性质变化的特点,建立低渗透油藏CO<sub>2</sub>驱试井解释改进模型,并运用数值差分方法进行求解。同时,综合SPSA优化搜索算法对压力曲线和压力导数曲线同时进行拟合,最终形成一套低渗透油藏CO<sub>2</sub>驱试井曲线自动拟合与参数解释方法。对矿场实际试井曲线解释参数变化规律进行分析,结果表明:考虑低渗透油藏特性对储层渗透率解释值有较大影响,优化后渗透率解释值比初始解释值增加了37.97%;而导压系数、压缩系数变化指数等相关参数解释值受流体分布非均质性影响程度较强,分别较初始解释值降低了16.94%和21.97%。矿场实际数据的应用效果显示,提出的试井解释方法可操作性强,适用性较好。

**关键词:**低渗透油藏;CO<sub>2</sub>驱;复合模型;曲线拟合;参数解释

中图分类号:TE353

文献标识码:A

## Well testing interpretation method for CO<sub>2</sub> flooding in low permeability oil reservoirs

SU Yuliang<sup>1</sup>, CAI Mingyu<sup>1</sup>, MENG Fankun<sup>2</sup>, FAN Liyao<sup>1</sup>, LI Lei<sup>1</sup>

(1. School of Petroleum Engineering, China University of Petroleum (East China), Qingdao City, Shandong Province, 266580, China; 2. Shengli College China University of Petroleum, Dongying City, Shandong Province, 257061, China)

**Abstract:** This paper focuses on the unknown problems of the well testing interpretation method for CO<sub>2</sub> flooding in low permeability oil reservoir. Based on the percolation theory of multi-region composite model, an improved model of well testing interpretation is developed, which is solved by the numerical differential method. In this model, the threshold pressure gradient, pressure sensitivity effect and fluid dynamic property during CO<sub>2</sub> flooding in the low permeability oil reservoir are considered. Meanwhile, Simultaneous Perturbation Stochastic Approximation (SPSA) optimum searching algorithm is conducted to fit pressure curve and pressure derivative curve simultaneously. Finally, automatic matching and parameter interpretation method of well testing for CO<sub>2</sub> flooding in the low permeability oil reservoir is proposed. The variation of interpretation parameters obtained from practical well testing curves is analyzed. The results show that consideration of low permeability characteristics would have an obvious influence on the interpretation of reservoir permeability, and the interpreted permeability after optimization is increased by 37.97% compared with the initial value. On the contrary, the interpreted pressure transmitting coefficient and compressibility variation index are decreased by 16.94% and 21.97% respectively from the original interpretations, which are considered to be influenced seriously by fluid heterogeneity. The applications reveal that the proposed interpretation method is easier to operate, and has good feasibility.

**Key words:** low permeability oil reservoirs; CO<sub>2</sub> flooding; composite model; curve matching; parameter interpretation

受制于低渗透油藏水驱注入能力,CO<sub>2</sub>驱已逐渐成为提高低渗透油藏采收率的主要方法之一,具

有广泛的应用前景<sup>[1-4]</sup>。在CO<sub>2</sub>注入过程中开展试井测试,可了解油藏性质及井的状况,对指导后续

收稿日期:2019-10-22。

作者简介:苏玉亮(1970—),男,山东东营人,教授,博士,从事非常规油气藏数值模拟与产能预测、注气提高采收率等研究。E-mail:suyuliang@upc.edu.cn。

基金项目:中国博士后基金“CO<sub>2</sub>吞吐提高页岩油采收率机理及数值模拟”(2018M630813)和“CO<sub>2</sub>吞吐提高页岩油采收率机理及CO<sub>2</sub>埋存效率研究”(2019T120616)。

生产具有重要意义<sup>[5-6]</sup>。目前,针对CO<sub>2</sub>驱,提出的多为复合油藏试井模型,TANG等率先揭示了CO<sub>2</sub>驱流体分布特征,将油藏划分为CO<sub>2</sub>区、CO<sub>2</sub>-原油过渡区及未波及原油区<sup>[7]</sup>;随后,AMBASTHA等建立了三区复合试井解释模型,分析试井曲线变化规律<sup>[8]</sup>,ISSAKA等假定过渡区流体性质为指数变化,给出了变性质过渡区复合模型半解析解<sup>[9]</sup>。在中国,王敬瑶运用传统三区复合模型,分析某CO<sub>2</sub>驱区块试井数据,但未考虑CO<sub>2</sub>驱流体分布特征<sup>[10]</sup>;朱建伟等基于两区复合模型,考虑流体性质变化所产生压降,但试井曲线无明显变化规律<sup>[11]</sup>;苏玉亮等充分考虑了CO<sub>2</sub>驱替过程中流体幂律型、非连续型等变化方式,建立了三区复合模型,分析其对试井曲线的影响<sup>[12-14]</sup>。近年来,众多学者又考虑应力敏感、水平井、垂直裂缝直井等复杂条件,建立多区复合模型,研究试井曲线变化特征<sup>[15-17]</sup>。

针对目前研究集中于试井曲线分析,而缺乏对CO<sub>2</sub>驱试井解释方法研究的现状,考虑启动压力梯度、应力敏感等低渗透油藏特性以及流体性质变化,建立改进复合区试井模型,并综合SPSA自动搜索优化算法,最终形成CO<sub>2</sub>驱试井解释方法流程。

## 1 CO<sub>2</sub>驱试井模型建立与求解

### 1.1 物理模型

由封闭边界低渗透油藏CO<sub>2</sub>驱三区复合模型剖面(图1)可见,一区为驱替波及区(CO<sub>2</sub>区);二区为CO<sub>2</sub>-原油过渡区(CO<sub>2</sub>+原油轻组分),该区流体性质与流体组分及油藏压力、温度等紧密相关,难以用特定函数统一表征;三区代表驱替未波及区(原油区)。

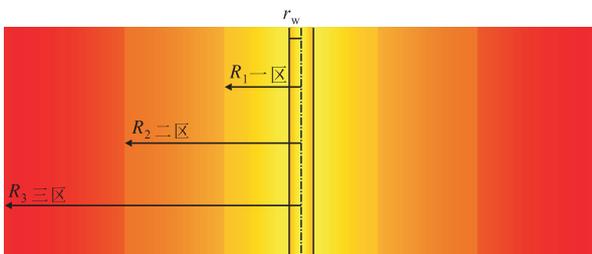


图1 低渗透油藏CO<sub>2</sub>驱三区复合模型剖面

Fig.1 Three-region composite model for CO<sub>2</sub> flooding in low permeability oil reservoir

一般地层条件下的温度和压力均超过CO<sub>2</sub>临界温度(304.14 K)和临界压力(7.382 MPa),故注入CO<sub>2</sub>实际处于超临界状态,其性质类似于液体,因此可简化模型为单相渗流。同时考虑低渗透油藏非达西渗流的特点,在模型中加入表征低渗透特点的

启动压力梯度及地层压力敏感性。模型的基本假设条件如下:①地层为水平、等厚且恒温的封闭地层,油藏原始地层压力在各处相等。②注入井CO<sub>2</sub>注入量恒定。③忽略重力和毛管力的影响,考虑表皮污染和井筒存储效应。④一区、三区中流体均微可压缩,且流体性质均一。⑤二区中流体黏度及压缩系数随半径呈连续(幂律、指数)、非连续等多种变化形式。⑥整个流动过程为单相渗流,受流体性质差别影响,各区启动压力梯度不同,均服从非达西渗流规律,渗流速度表达式为:

$$v = -\frac{K}{\mu}(\nabla p - G) \quad (1)$$

⑦考虑CO<sub>2</sub>注入过程中地层压敏效应,其渗透率变化可表示为:

$$\varepsilon = \frac{1}{K} \times \frac{dK}{dp} \quad (2)$$

### 1.2 数学模型

根据物理模型的假设,推导渗流数学模型并进行无因次化后可得:

$$\left\{ \begin{aligned} & \frac{\partial^2 p_{1D}}{\partial r_D^2} - \varepsilon_{1D} \left( \frac{\partial p_{1D}}{\partial r_D} \right)^2 + \left( \frac{1}{r_D} - G_{1D} \varepsilon_D e^{-s} \right) \frac{\partial p_{1D}}{\partial r_D} + \frac{G_{1D} e^{-s}}{r_D} = e^{(\varepsilon_{1D} p_D - 2s)} \frac{\partial p_{1D}}{\partial t_D} & 1 < r_D < R_{1D} \\ & \frac{\partial^2 p_{2D}}{\partial r_D^2} - \varepsilon_{2D} \left( \frac{\partial p_{2D}}{\partial r_D} \right)^2 + \left( \frac{1}{r_D} - G_{2D} \varepsilon_{2D} e^{-s} - V \right) \times \\ & \left\{ \frac{\partial p_{2D}}{\partial r_D} + \frac{G_{2D} e^{-s}}{r_D} (1 - V) = \eta_{12} W Q e^{(\varepsilon_{2D} p_D - 2s)} \times \frac{\partial p_{2D}}{\partial t_D} \right. & R_{1D} < r_D < R_{2D} \\ & \frac{\partial^2 p_{3D}}{\partial r_D^2} - \varepsilon_{3D} \left( \frac{\partial p_{3D}}{\partial r_D} \right)^2 + \left( \frac{1}{r_D} - G_{3D} \varepsilon_D e^{-s} \right) \frac{\partial p_{3D}}{\partial r_D} + \frac{G_{3D} e^{-s}}{r_D} = \eta_{13} e^{(\varepsilon_{3D} p_D - 2s)} \frac{\partial p_{3D}}{\partial t_D} & R_{2D} < r_D < R_{3D} \end{aligned} \right. \quad (3)$$

模型边界条件为:

$$\left\{ \begin{aligned} & \left( \frac{\partial p_{1D}}{\partial r_D} + G_{1D} e^{-s} \right) = e^{\varepsilon_{1D} p_{1D}} \Big|_{r_D=1} \left( 1 + C_D \frac{dp_{wD}}{dt_D} \right) & r_D = 1 \\ & \frac{\partial p_{2D}}{\partial r_D} + G_{2D} e^{-s} = M_{12} \left( \frac{\partial p_{1D}}{\partial r_D} + G_{1D} e^{-s} \right) & r_D = R_{1D} \\ & \frac{\partial p_{2D}}{\partial r_D} + G_{2D} e^{-s} = M_{23} \left( \frac{\partial p_{1D}}{\partial r_D} + G_{1D} e^{-s} \right) & r_D = R_{2D} \\ & \frac{\partial p_{3D}}{\partial r_D} + G_{3D} e^{-s} = 0 & r_D = R_{3D} \end{aligned} \right. \quad (4)$$

模型初始条件为:

$$\begin{cases} p_{1D} = p_{2D} = p_{3D} = 0 \\ t_D = 0 \end{cases} \quad (5)$$

(3)式中,在  $R_{1D} < r_D < R_{2D}$  的条件下,  $V, W, Q$  的定义式分别为:

$$V = \frac{1}{\mu_2} \times \frac{\partial \mu_2}{\partial r_D} \quad (6)$$

$$W = \frac{C_{2t}}{C_{2t}|_{r_D=R_{1D}}} \quad (7)$$

$$Q = \frac{\mu_2}{\mu_2|_{r_D=R_{1D}}} \quad (8)$$

当黏度及压缩系数随半径成解析函数形式变化时,对于给定的  $r_D$  可以直接计算出该半径处的  $V, W, Q$  值;对于黏度及压缩系数随半径成不规则变化时,对于给定的  $r_D$  可以采用插值法(如样条插值)计算出该半径处的  $V, W, Q$  值。

(3)—(8)式中其他各无因次参数定义式为:

$$p_{1D} = \frac{2\pi K_1 h}{q\mu_1 B_g} (p_i - p_1) \quad (9)$$

$$p_{2D} = \frac{2\pi K_1 h}{q\mu_1 B_g} (p_i - p_2) \quad (10)$$

$$p_{3D} = \frac{2\pi K_1 h}{q\mu_1 B_g} (p_i - p_3) \quad (11)$$

$$p_{wD} = \frac{2\pi K_1 h}{q\mu_1 B_g} (p_i - p_w) \quad (12)$$

$$\eta_{12} = \frac{\left(\frac{K}{\phi\mu C_1}\right)_1}{\left(\frac{K}{\phi\mu C_1}\right)_2|_{r_D=R_{1D}}} \quad (13)$$

$$\eta_{13} = \frac{\left(\frac{K}{\phi\mu C_1}\right)_1}{\left(\frac{K}{\phi\mu C_1}\right)_3} \quad (14)$$

$$M_{12} = \frac{\left(\frac{K}{\mu}\right)_1}{\left(\frac{K}{\mu}\right)_2|_{r_D=R_{1D}}} \quad (15)$$

$$M_{23} = \frac{\left(\frac{K}{\mu}\right)_2}{\left(\frac{K}{\mu}\right)_3}|_{r_D=R_{2D}} \quad (16)$$

$$t_D = \frac{K_1 t}{(\mu C_1 \phi)_1 r_w^2} \quad (17)$$

$$r_D = \frac{r}{r_w e^{-s}} \quad (18)$$

$$C_D = \frac{C}{2\pi\phi_1 C_{1t} h r_w^2} \quad (19)$$

$$G_{1D} = \frac{2\pi K_1 h r_w G_1}{q\mu_1 B_g} \quad (20)$$

$$G_{2D} = \frac{2\pi K_1 h r_w G_2}{q\mu_1 B_g} \quad (21)$$

$$G_{3D} = \frac{2\pi K_1 h r_w G_3}{q\mu_1 B_g} \quad (22)$$

$$\varepsilon_{1D} = \frac{q\mu_1 B_g \varepsilon_1}{2\pi K_1 h} \quad (23)$$

$$\varepsilon_{2D} = \frac{q\mu_1 B_g \varepsilon_2}{2\pi K_1 h} \quad (24)$$

$$\varepsilon_{3D} = \frac{q\mu_1 B_g \varepsilon_3}{2\pi K_1 h} \quad (25)$$

### 1.3 模型求解

借鉴文献[14]中所采用的求解方法,首先对渗流方程及边界条件((1)—(4)式)进行对数坐标的转化,并对主控方程((3)式)进行离散可得:

$$\begin{aligned} & a(i) p_{Di-1}^j + b(i) p_{Di}^j + c(i) p_{Di+1}^j + d(i) (p_{Di}^j)^2 + \\ & e(i) p_{Di}^j p_{Di+1}^j + f(i) (p_{Di+1}^j)^2 + g(i) e^{\varepsilon_D p_{Di}^j} + \\ & h(i) p_{Di}^j e^{\varepsilon_D p_{Di}^j} + k(i) = 0 \end{aligned} \quad (26)$$

设一区、二区及三区网格数分别为  $N_1, N_2, N_3$ , 则对于一区  $1 < i < N_1$ :

$$\left\{ \begin{aligned} a(i) &= \frac{1}{\Delta x^2} \\ b(i) &= -\frac{2}{\Delta x^2} + \frac{G_{1D}e^{-s}\varepsilon_{1D}e^{(i-1)\Delta x}}{\Delta x} \\ c(i) &= \frac{1}{\Delta x^2} - \frac{G_{1D}e^{-s}\varepsilon_{1D}e^{(i-1)\Delta x}}{\Delta x} \\ d(i) &= -\frac{\varepsilon_{1D}}{\Delta x^2} \\ e(i) &= \frac{2\varepsilon_{1D}}{\Delta x^2} \\ f(i) &= -\frac{\varepsilon_{1D}}{\Delta x^2} \\ g(i) &= \frac{e^{2(i-1)\Delta x} p_{D1}^{j-1}}{e^{2s}\Delta t_D} \\ h(i) &= \frac{e^{2(i-1)\Delta x}}{e^{2s}\Delta t_D} \\ k(i) &= G_{1D}e^{-s}e^{(i-1)\Delta x} \end{aligned} \right. \quad (27)$$

对于二区  $N_1 < i < N_2$ :

$$\left\{ \begin{aligned} a(i) &= \frac{1}{\Delta x^2} \\ b(i) &= -\frac{2}{\Delta x^2} + \frac{G_{2D}e^{-s}\varepsilon_{2D}e^{(i-1)\Delta x}}{\Delta x} + \frac{V(i)e^{(i-1)\Delta x}}{\Delta x} \\ c(i) &= \frac{1}{\Delta x^2} - \frac{G_{2D}e^{-s}\varepsilon_{2D}e^{(i-1)\Delta x}}{\Delta x} - \frac{V(i)e^{(i-1)\Delta x}}{\Delta x} \\ d(i) &= -\frac{\varepsilon_{2D}}{\Delta x^2} \\ e(i) &= \frac{2\varepsilon_{2D}}{\Delta x^2} \\ f(i) &= -\frac{\varepsilon_{2D}}{\Delta x^2} \\ g(i) &= W(i)Q(i)\eta_{12} \frac{e^{2(i-1)\Delta x} p_{2D1}^{j-1}}{e^{2s}\Delta t_D} \\ h(i) &= -W(i)Q(i)\eta_{12} \frac{e^{2(i-1)\Delta x}}{e^{2s}\Delta t_D} \\ k(i) &= G_{2D}e^{-s}e^{(i-1)\Delta x} \end{aligned} \right. \quad (28)$$

对于三区  $N_2 < i < N_3$ :

$$\left\{ \begin{aligned} a(i) &= \frac{1}{\Delta x^2} \\ b(i) &= -\frac{2}{\Delta x^2} + \frac{G_{3D}e^{-s}\varepsilon_{3D}e^{(i-1)\Delta x}}{\Delta x} \\ c(i) &= \frac{1}{\Delta x^2} - \frac{G_{3D}e^{-s}\varepsilon_{3D}e^{(i-1)\Delta x}}{\Delta x} \\ d(i) &= -\frac{\varepsilon_{3D}}{\Delta x^2} \\ e(i) &= \frac{2\varepsilon_{3D}}{\Delta x^2} \\ f(i) &= -\frac{\varepsilon_{3D}}{\Delta x^2} \\ g(i) &= \eta_{23} \frac{e^{2(i-1)\Delta x} p_{3D1}^{j-1}}{e^{2s}\Delta t_D} \\ h(i) &= -\eta_{23} \frac{e^{2(i-1)\Delta x}}{e^{2s}\Delta t_D} \\ k(i) &= G_{3D}e^{-s}e^{(i-1)\Delta x} \end{aligned} \right. \quad (29)$$

内边界 ( $i=1$ ) 离散为:

$$\begin{aligned} b(1) p_{1D1}^j + c(1) p_{1D2}^j + g(1) e^{\varepsilon_{1D} p_{1D1}^j} + \\ h(1) p_{D1}^j e^{\varepsilon_{1D} p_{1D1}^j} + k(1) = 0 \end{aligned} \quad (30)$$

其中:

$$\left\{ \begin{aligned} b(1) &= -\frac{1}{\Delta x} \\ c(1) &= \frac{1}{\Delta x} \\ g(1) &= 1 + \frac{C_D p_{1D1}^j}{\Delta t_D} \\ h(1) &= -\frac{C_D}{\Delta t_D} \\ k(1) &= G_{1D}e^{-s} \end{aligned} \right. \quad (31)$$

一区-二区 ( $i=N_1$ )、二区-三区 ( $i=N_2$ ) 交界面及外边界 ( $i=N_3$ ) 离散方程分别为:

$$\begin{aligned} p_{D_{i-1}}^j - \left(1 + \frac{1}{M_{12}}\right) p_{Di}^j + \frac{1}{M_{12}} p_{D_{i+1}}^j + \\ \Delta x e^{(i-1)\Delta x} \left( \frac{G_{2D}e^{-s} - G_{1D}e^{-s}}{M_{12}} \right) = 0 \end{aligned} \quad (32)$$

$$\begin{aligned} p_{D_{i-1}}^j - \left(1 + \frac{1}{M_{23}}\right) p_{Di}^j + \frac{1}{M_{23}} p_{D_{i+1}}^j + \\ \Delta x e^{(i-1)\Delta x} \left( \frac{G_{3D}e^{-s} - G_{2D}e^{-s}}{M_{23}} \right) = 0 \end{aligned} \quad (33)$$

$$p_{Di}^j - p_{D_{i-1}}^j + \Delta x e^{(i-1)\Delta x} G_{3D}e^{-s} = 0 \quad (34)$$

对(27)–(30), (32)–(34)式进行统一整理, 可得到线性代数方程组:

$$F = \begin{cases} f_1(p_{1D1}, p_{1D2}) = 0 \\ f_2(p_{1D1}, p_{1D2}, p_{1D3}) = 0 \\ f_3(p_{1D2}, p_{1D3}, p_{1D4}) = 0 \\ \vdots \\ f_{N_1}(p_{1DN_1-1}, p_{DN_1}, p_{2DN_1+1}) = 0 \\ \vdots \\ f_{N_2}(p_{2DN_2-1}, p_{DN_2}, p_{3DN_2+1}) = 0 \\ \vdots \\ f_n(p_{3DN-1}, p_{3DN}, p_{3DN+1}) = 0 \\ f_{N_3}(p_{3DN_3-1}, p_{3DN_3}) = 0 \end{cases} \quad (35)$$

利用 Newton-Raphson 方法构造牛顿迭代矩阵:

$$J \cdot P = -F \quad (36)$$

即可求解关于压力的非线性方程组:

$$P^{j+1} = P^j + \Delta P^{j+1} \quad (37)$$

## 2 SPSA 搜索优化算法

SPSA (Simultaneous Perturbation Stochastic Approximation) 方法最先由 SPALL<sup>[18]</sup>于 1992 年提出,与传统的有限差分近似法(梯度法)不同,该方法通过设置一定的随机变量,对所有控制变量进行同步扰动,以此来获得扰动梯度,进行损失函数等性能指标函数的计算。尽管扰动梯度是随机的,但通过选择适当的随机变量,可以保证对于最小化问题来讲恒为下山方向,且期望值为真实梯度。算法的计算流程包括以下 6 个步骤<sup>[19]</sup>:①模型参数初始化及选择。设定计数标记  $k=0$ 。选择初始估计值  $\theta_0$ , 根据迭代系数  $\alpha_k$  和  $c_k$  计算表达式 ( $\alpha_k = a/(A+k+1)$ ,  $c_k = c/(k+1)^\gamma$ ), 确定非负系数  $a, c, A, \alpha$  和  $\gamma$ 。②随机扰动向量生成。运用 Bernoulli $\pm 1$  分布生成  $p$  维扰动向量  $\Delta k$ , 为提高早期迭代稳定性,采用多次计算后的平均梯度。③目标函数估计。基于目前值  $\hat{\theta}_k$  附近的同步扰动,根据步骤①和②中设定的  $c_k$  与  $\Delta_k$ , 计算两者目标函数值  $y(\hat{\theta}_k + c_k \Delta_k)$  和  $y(\hat{\theta}_k - c_k \Delta_k)$ 。④梯度的近似计算。生成同步扰动变化梯度,其表达式为:

$$g_k(\hat{\theta}_k) = \frac{y(\hat{\theta}_k + c_k \Delta_k) - y(\hat{\theta}_k - c_k \Delta_k)}{2c_k} \begin{bmatrix} \Delta_{k1}^{-1} \\ \Delta_{k2}^{-1} \\ \vdots \\ \Delta_{kp}^{-1} \end{bmatrix} \quad (38)$$

$g_k(\hat{\theta}_k)$  中  $p$  个变量反映  $\hat{\theta}_k$  中所有元素同步扰动;⑤参数迭代更新。对  $\hat{\theta}_k$  进行更新的表达式为:

$$\hat{\theta}_{k+1} = \hat{\theta}_k - \alpha_k g_k(\hat{\theta}_k) \quad (39)$$

⑥迭代终止条件判断。返回到第②步,运用  $k+1$  代替  $k$ 。当相邻 2 次迭代步骤间计算结果差值较小,满

足设定阈值,或达到最大迭代步数时终止运算。

## 3 试井解释与自动拟合方法

对于低渗透油藏 CO<sub>2</sub> 驱的试井解释,商业试井软件不易考虑其低渗透及 CO<sub>2</sub> 驱的特性。因此,可构建低渗透油藏 CO<sub>2</sub> 驱试井解释自动拟合方法,其基本思路为:先通过常规试井解释方法得到初始参数值,再通过自动搜索算法结合改进的模型进行拟合矫正。其具体流程如下:①拟定初始解释参数,可采用常规试井解释软件,得到基于均质复合区模型的解释值作为初始值。②根据矿场、实验或者数值模拟数据,给定启动压力梯度、压敏系数以及过渡区参数的变化形式。③根据上述参数重新计算压力及压力导数曲线。④计算目标函数。⑤利用 SPSA 算法在变量定义域 ( $\mathbf{x}_{\min}, \mathbf{x}_{\max}$ ) 中进行搜索,使得目标函数值最小。⑥调整搜索步长和搜索次数,使所求的  $\mathbf{x}$  满足精度要求,并符合实际情况。⑦绘制优化后的压力及压力导数曲线图。

目标函数为:

$$D(\mathbf{x}) = \sum_{i=1}^n [p(\mathbf{x}, t_{Di}) - p(t_{Di})]^2 + \sum_{i=1}^n \left[ \frac{dp}{d \ln t(\mathbf{x}, t_{Di})} - \frac{dp}{d \ln t(t_{Di})} \right]^2 \quad (40)$$

目标函数采用的是对压力曲线和压力导数曲线同时进行拟合。由于目前已有的低渗透油藏 CO<sub>2</sub> 实际试井数据极为有限,因此这里采用文献[3]中 CO<sub>2</sub> 试井数据进行算例示范操作。在该实例中,因采用压力恢复试井,测试压力随时间的增长而增大,初始增大速率较小,后期逐步稳定,由于 3 个区间存在界面,使得压力增大速率出现局部突变。通过商业软件采用二区复合油藏模型(表 1)初步拟合参数,初步试井参数解释结果为:半径为 31.3 m,表皮系数为 2.72,井储系数为 0.004 4,流度比为 1.09,导压系数为 0.37,渗透率为 31.3 mD,指数  $I$  为 0.7,所得初始拟合曲线见图 2。

将基础数据及初始值导入自动拟合程序。假设该油藏为低渗透油藏,且注二氧化碳时启动压力梯度为 0.01 MPa/m,地层压敏系数为 0.1 mD/MPa。同时,假定在上述二区模型中存在过渡带。由初步试井参数解释结果可以看出,两区流度比值相差较小,因此黏度的变化在此算例中忽略不计,仍设为恒定值。在过渡区域内压缩系数的变化可简化为呈指数形式变化(由组分模型计算归纳得到),即:

表1 油藏参数  
Table1 Reservoir parameters

参数	数值	参数	数值
孔隙度	0.185	CO <sub>2</sub> 井底黏度(mPa·s)	0.067
厚度(m)	9.144	井筒半径(m)	0.1
原油压缩系数(MPa <sup>-1</sup> )	1.02×10 <sup>-3</sup>	总CO <sub>2</sub> 注入量(m <sup>3</sup> )	889 147.52
平均CO <sub>2</sub> 压缩系数(MPa <sup>-1</sup> )	1.86×10 <sup>-2</sup>	CO <sub>2</sub> 体积系数(m <sup>3</sup> /m <sup>3</sup> )	0.002 459
地层压缩系数(MPa <sup>-1</sup> )	1.89×10 <sup>-3</sup>	平均注入天数(d)	31
水压缩系数(MPa <sup>-1</sup> )	4.35×10 <sup>-4</sup>	估算含水饱和度	0.75
最终CO <sub>2</sub> 日注入量(m <sup>3</sup> /d)	44 627.28	估算含油饱和度	0.25

$$C_t = C_t^o r_D^{-1} \quad (41)$$

此时所得优化前曲线见图2。

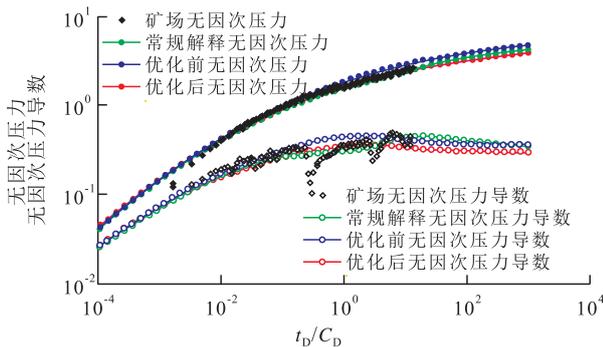


图2 优化曲线前后对比

Fig.2 Comparison of curves before and after optimization

由于所需搜索的各个参数在数量级以及数值上具有较大差异,因此,为了减小搜索范围,提高搜索速度,采用对各参数的变化倍数进行搜索的方法。即初始搜索值为全为1的向量。根据油藏实际,可给定参数变化倍数的上下限。最终优化所得曲线见图2,其最小二乘值变化如图3所示。

根据最终优化的向量,可得出优化后的数值

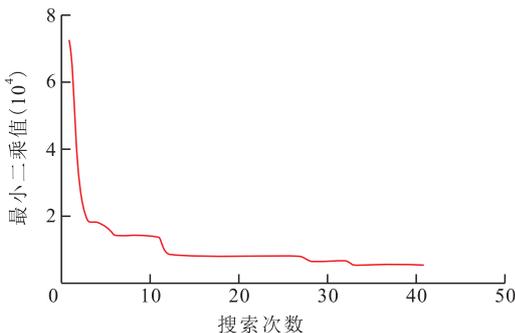


图3 优化过程中最小二乘值变化

Fig.3 Change of target least-square value during optimization

(表2)。由表2可见,在该算例中,渗透率、井储系数、导压系数以及指数I的变化最为明显。除了井储系数,其余参数都与油藏低渗透特性及非均质流体有直接关系。当存在启动压力梯度及压敏效应时,理论曲线会向上抬高;而渗透率增大时,会使理论曲线相对下降。因此优化后,渗透率解释值增大。而当考虑非均质压缩系数流体时,指数I与导压系数与其直接相关,因此其参数解释值变化较大。

表2 优化后参数变化值  
Table2 Parameters after optimization

参数	R(m)	S	C(cm <sup>3</sup> /10 <sup>-1</sup> MPa)	M	η	K(mD)	I
优化值	30.24	2.58	0.003 4	1.21	0.31	43.18	0.55
变化值(%)	3.39	5.28	23.64	11.91	16.94	37.97	21.97

## 4 结论

考虑低渗透油藏CO<sub>2</sub>驱替过程中存在启动压力梯度以及压敏效应的特点,同时对CO<sub>2</sub>驱所导致的流体性质变化运用解析或插值函数进行描述,建立了低渗透油藏CO<sub>2</sub>驱非均质流体三区复合模型,并进行了数值求解。

基于改进的复合模型,结合SPSA搜索优化算法,形成了一套低渗透油藏CO<sub>2</sub>驱试井解释方法,并对实际数据进行了算例计算。

参数修正解释结果表明,当考虑低渗透油藏低渗透特性时,对储层渗透率的参数解释影响较大;当考虑流体非均质分布时,与之相关的指数系数和导压系数等的参数解释值会受到较大影响。

### 符号解释

$r_w$ ——井筒原始半径,cm; $R$ ——区域半径,m;下标1,2,3——一区、二区和三区; $v$ ——流体渗流速度,cm/s; $K$ ——地层渗透率,mD; $\mu$ ——流体黏度,mPa·s; $\nabla p$ ——压力梯度,10<sup>-1</sup> MPa/cm; $G$ ——启动压力梯度,10<sup>-1</sup> MPa/cm; $\varepsilon$ ——压敏系数,10<sup>-1</sup> MPa/cm; $p$ ——压力,10<sup>-1</sup> MPa;下标D——无因次; $r$ ——储层径向半径,cm; $S$ ——井筒表皮系数; $t$ ——时间,s; $V, W, Q$ ——表征区域二中流体性质变化的中间变量,无因次; $\eta_{12}, \eta_{13}$ ——一区和二区、一区和三区导压系数比; $C$ ——井储系数,cm<sup>3</sup>/10<sup>-1</sup> MPa; $p_w$ ——井底压力,10<sup>-1</sup> MPa; $M_{12}, M_{23}$ ——一区和二区、二区和三区流体流量比; $C_t$ ——地层压缩系数,10 MPa<sup>-1</sup>; $h$ ——地层厚度,cm; $q$ ——注入量,cm<sup>3</sup>/s; $B_g$ ——注入流体的体积系数,cm<sup>3</sup>/cm<sup>3</sup>; $p_i$ ——原始地层压力,10<sup>-1</sup> MPa; $\phi$ ——地层孔隙度; $i$ ——网格数,1< $i$ < $N_3$ ; $j$ ——时间步; $x$ ——对数坐标转换结果, $x=\ln r$ ; $F$ ——残差矩阵; $J$ ——系数矩阵; $P$ ——压力矩阵; $g_k(\hat{\theta}_k)$ ——同步扰动变化梯度; $\hat{\theta}_k$ ——第k次迭代的估计值; $\Delta_{ki}$ ——向量 $\Delta_k$ 中的第i个

元素(可能是随机变量 $\pm 1$ ); $C_0^*$ ——一区外边界处的压缩系数,10 MPa<sup>-1</sup>;I——压缩系数变化指数,初始值设为0.7。

### 参考文献

- [1] 孟凡坤,苏玉亮,郝永卯,等.基于B-L方程的低渗透油藏CO<sub>2</sub>水气交替注入能力[J].中国石油大学学报:自然科学版,2018,42(4):91-99.  
MENG Fankun, SU Yuliang, HAO Yongmao, et al. Injectivity of CO<sub>2</sub> WAG in low permeability oil reservoirs based on B-L equations[J]. Journal of China University of Petroleum; Edition of Natural Science, 2018, 42(4): 91-99.
- [2] 孟凡坤,雷群,苏玉亮,等.低渗透油藏CO<sub>2</sub>非混相驱前缘移动规律研究[J].西南石油大学学报:自然科学版,2018,40(3):121-128.  
MENG Fankun, LEI Qun, SU Yuliang, et al. Law of CO<sub>2</sub> immiscible front movement in low-permeability oil reservoir [J]. Journal of Southwest Petroleum University: Science & Technology Edition, 2018, 40(3): 121-128.
- [3] 王洪峰,李晓平,王小培,等.多井干扰试井技术在克深气田勘探开发中的应用[J].油气地质与采收率,2018,25(1):100-105.  
WANG Hongfeng, LI Xiaoping, WANG Xiaopei, et al. Application of multi-well interference test technology in exploration and development of Keshen Gasfield[J]. Petroleum Geology and Recovery Efficiency, 2018, 25(1): 100-105.
- [4] 祝浪涛,廖新维,陈志明,等.应力敏感性低渗透油藏CO<sub>2</sub>混相驱试井模型[J].油气地质与采收率,2017,24(4):88-93.  
ZHU Langtao, LIAO Xinwei, CHEN Zhiming, et al. Well test model of CO<sub>2</sub> miscible flooding in the low-permeability reservoirs with stress sensitivity [J]. Petroleum Geology and Recovery Efficiency, 2017, 24(4): 88-93.
- [5] 姜瑞忠,张福蕾,杨明,等.双重介质低渗透油藏水平井试井模型[J].特种油气藏,2019,26(3):79-84.  
JIANG Ruizhong, ZHANG Fulei, YANG Ming, et al. Horizontal well test model of dual-medium low-permeability reservoir [J]. Special Oil & Gas Reservoirs, 2019, 26(3): 79-84.
- [6] 曾杨,康晓东,唐恩高,等.水驱后聚驱双层复合油藏试井解释[J].大庆石油地质与开发,2018,37(6):60-66.  
ZENG Yang, KANG Xiaodong, TANG Engao, et al. Well test interpretation of the polymer-flooded double-layer composite oil reservoir after water displaced [J]. Petroleum Geology & Oilfield Development in Daqing, 2018, 37(6): 60-66.
- [7] TANG R W, AMBASTHA A K. Analysis of CO<sub>2</sub> pressure transient data with two-and three-region analytical radial composite model [R]. SPE 18275, 1988: 143-152.
- [8] AMBASTHA A K, JR RAMERY H J. Pressure transient analysis for a three region composite reservoir [R]. SPE 24378, 1992: 589-598.
- [9] ISSAKA M, AMBASTHA A K. An improved three-region composite reservoir model for thermal recovery well test analysis [C]. Toronto: Annual Technical Meeting, Petroleum Society of Canada, 1997.
- [10] 王敬瑶.二氧化碳驱试验区试井测试资料分析及应用[J].大庆石油学院学报,2011,35(3):85-90.  
WANG Jingyao. Analysis of well testing data of carbon dioxide flooding zone and its application [J]. Journal of Daqing Petroleum Institute, 2011, 35(3): 85-90.
- [11] 朱建伟,邵长金,廖新维,等.注二氧化碳混相驱试井模型及压力分析[J].油气井测试,2011,20(4):1-4.  
ZHU Jianwei, SHAO Changjin, LIAO Xinwei, et al. Miscible flooding well test model with carbon dioxide injection and its pressure analysis [J]. Well Testing, 2011, 20(4): 1-4.
- [12] 苏玉亮,孟凡坤,周诗雨,等.低渗透油藏CO<sub>2</sub>驱试井曲线特征分析[J].科技导报,2015,33(18):34-39.  
SU Yuliang, MENG Fankun, ZHOU Shiyu, et al. Characteristics analysis of well testing curve of CO<sub>2</sub> flooding in low permeability reservoir [J]. Science & Technology Review, 2015, 33(18): 34-39.
- [13] 李友全,孟凡坤,阎燕,等.考虑流体非均质性的低渗透油藏CO<sub>2</sub>驱试井分析[J].岩性油气藏,2016,28(4):106-112.  
LI Youquan, MENG Fankun, YAN Yan, et al. Pressure transient analysis on CO<sub>2</sub> flooding in low permeability reservoirs considering fluid heterogeneity [J]. Lithologic Reservoirs, 2016, 28(4): 106-112.
- [14] 李友全,韩秀虹,阎燕,等.低渗透油藏CO<sub>2</sub>吞吐压力响应曲线分析[J].岩性油气藏,2017,29(6):119-127.  
LI Youquan, HAN Xiuhong, YAN Yan, et al. Pressure transient analysis on CO<sub>2</sub> huff and puff in low permeability reservoir [J]. Lithologic Reservoirs, 2017, 29(6): 119-127.
- [15] 刘启国,刘丹,朱晨曦,等.致密砂岩垂直裂缝井CO<sub>2</sub>混相驱试井模型研究[J].力学季刊,2018,39(3):615-621.  
LIU Qiguo, LIU Dan, ZHU Chenxi, et al. Study of well test model on CO<sub>2</sub> miscible flooding in the tight sand reservoirs with fractured well [J]. Chinese Quarterly of Mechanics, 2018, 39(3): 615-621.
- [16] 姜瑞忠,张海涛,张伟,等.CO<sub>2</sub>驱三区复合油藏水平井压力动态分析[J].油气地质与采收率,2018,25(6):63-70.  
JIANG Ruizhong, ZHANG Haitao, ZHANG Wei, et al. Dynamic pressure analysis of three-zone composite horizontal well in oil reservoirs for CO<sub>2</sub> flooding [J]. Petroleum Geology and Recovery Efficiency, 2018, 25(6): 63-70.
- [17] 阎燕,李友全,于伟杰,等.低渗透油藏CO<sub>2</sub>驱采油井试井模型[J].断块油气田,2018,25(1):80-84.  
YAN Yan, LI Youquan, YU Weijie, et al. Well test model research for CO<sub>2</sub> flooding production well in low permeability reservoirs [J]. Fault-Block Oil & Gas Field, 2018, 25(1): 80-84.
- [18] SPALL J C. Multivariate stochastic approximation using a simultaneous perturbation gradient approximation [J]. IEEE Transactions on Automatic Control, 1992, 37(3): 332-341.
- [19] SPALL J C. Implementation of the simultaneous perturbation algorithm for stochastic optimization [J]. IEEE Transactions on Aerospace and Electronic Systems, 1998, 34(3): 817-823.